Design of Highly Selective Microstrip Bandpass Filters with a Single Pair of Attenuation Poles at Finite Frequencies

Jia-Sheng Hong, *Member, IEEE,* and Michael J. Lancaster, *Member, IEEE*

***Abstract*—This paper presents the design of a class of highly selective microstrip bandpass filters that consist of microstrip open-loop resonators that exhibit a single pair of attenuation poles at finite frequencies. A practical design technique for this class of filters is introduced, including tables and formulas for accurate and fast filter synthesis. Two design examples of a six-pole filter with a fractional bandwidth of 7.331% at 955 MHz and an eight-pole filter with a fractional bandwidth of 10.359% at 985 MHz are described. Theoretical and experimental results are presented. The compact size and the excellent performance of this class of filters have been demonstrated.**

***Index Terms*—Microstrip filters, microstrip resonators, microwave bandpass filters.**

I. Introduction

RAPID development of wireless communications present extraordinary demand for narrow-band RF/microwave bandpass filters with high selectivity and low insertion loss. One filter with these attractive characteristics is that of quasi-elliptic function response filters with a pair of attenuation poles at finite frequencies [1]–[2]. The capability of placing attenuation poles near the cutoff frequencies of the passband improves the selectivity using less resonators. This type of filter is usually realized using waveguide cavities or dielectric-resonator-loaded cavities. However, with the advent of high-temperature superconducting (HTS) and micromachined circuit technologies, there is an increasing interest in microstrip filter structures [3]–[10]. Two technical approaches are normally used to realize this type of filter. The first is to extract poles from both ends of a filter prototype by using shunt resonators [4]. The size of the microstrip filter resulting from this approach may, however, be large. The second approach is to introduce a cross coupling between a pair of nonadjacent resonators [5]–[10]. The filter employing the cross coupling generally results in a compact topology. This is obviously more attractive for those systems where size is important.

It has been known that the cross coupling is more difficult to be arranged and controlled in a microstrip filter owing to its semiopen structure. Even a recent paper [10] only reported the design of a two-pole microstrip filter with a crossing line for the cross coupling. It is obvious, however, that a higher degree is required for a more selective filter. In this paper, we present in detail the design of highly selective microstrip bandpass filters that consist of microstrip open-loop resonators with a cross coupling that exhibit a single pair of attenuation poles at finite frequencies. A practical design technique for this class of filters, which is also different from that reported in [10], is introduced, including tables and formulas for accurate and fast filter synthesis. The design approach enables one to use advanced full-wave EM simulators to complete the filter design, namely, to determine the physical dimensions of the filter. Two design examples of six- and eight-pole filters are demonstrated together with theoretical and experimental results.

Manuscript received October 21, 1998.

The authors are with the School of Electronic and Electrical Engineering, University of Birmingham, Edgbaston, Birmingham B15 2TT, U.K.

Publisher Item Identifier S 0018-9480(00)05466-1.

II. Filter Characteristics and Configurations

Let us consider a transfer function

$$|S_{21}(\Omega)|^2 = \frac{1}{1+\varepsilon^2 F_N^2(\Omega)} \tag{1}$$

where Ω is the frequency variable that is normalized to the passband cutoff frequency of a low-pass prototype filter, ε is a ripple constant related to a given return loss L_R in decibels by

$$\varepsilon = \frac{1}{\sqrt{10^{-(L_R/10)}-1}}. \tag{2}$$

The form of $F_N(\Omega)$ for the selective filters considered may be expressed as [11]

$$F_N(\Omega) = \cosh\left\{(N-2)\cosh^{-1}(\Omega) + \cosh^{-1}\left(\frac{\Omega_a\Omega-1}{\Omega_a-\Omega}\right) + \cosh^{-1}\left(\frac{\Omega_a\Omega+1}{\Omega_a+\Omega}\right)\right\} \tag{3}$$

so that $\Omega = \pm\Omega_a$ ($\Omega_a > 1$) are the frequency locations of a pair of attenuation poles. Note that if $\Omega_a \to \infty$, the function $F_N(\Omega)$ degenerates to the familiar Chebyshev function and the frequency response of (1) will be a pure Chebyshev filter response. The transmission frequency response of the bandpass filter may be determined using the following frequency mapping

$$\Omega = \frac{1}{\mathrm{FBW}} \cdot \left(\frac{\omega}{\omega_0} - \frac{\omega_0}{\omega}\right) \tag{4}$$

in which ω is the frequency variable of bandpass filter, ω_0 is the midband frequency, and FBW is the fractional bandwidth.

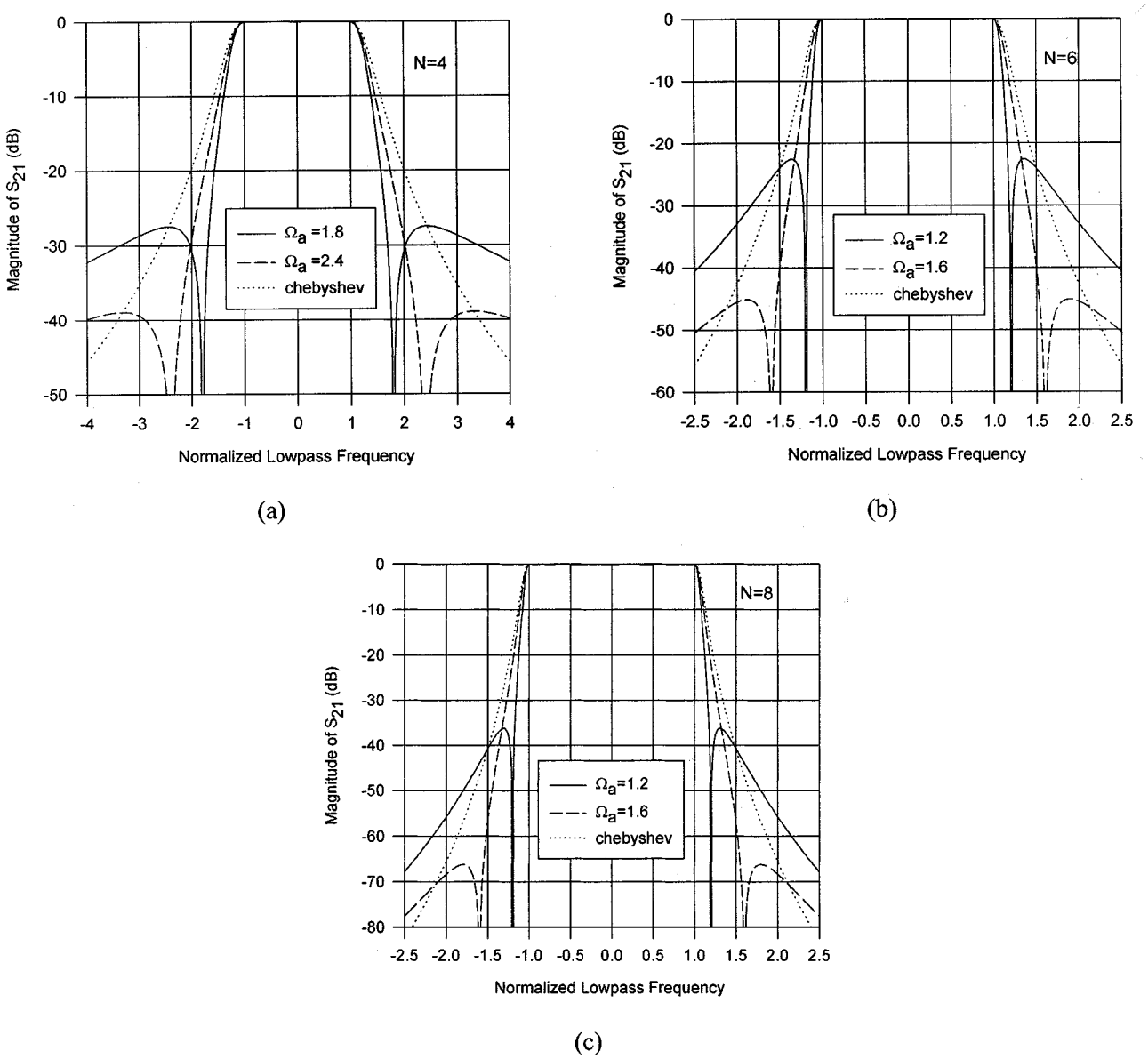

Fig. 1. Comparison of frequency responses of the Chebyshev filter and the filter with a single pair of attenuation poles at finite frequencies. (a) Four-pole ($N = 4$). (b) Six-pole ($N = 6$). (c) Eight-pole ($N = 8$).

The locations of two finite frequency attenuation poles of the bandpass filter, namely, ω_{a1} and ω_{a2}, are given by

$$\omega_{a1} = \omega_0 \frac{-\Omega_a \mathrm{FBW} + \sqrt{(\Omega_a \mathrm{FBW})^2 + 4}}{2}$$
$$\omega_{a2} = \omega_0 \frac{\Omega_a \mathrm{FBW} + \sqrt{(\Omega_a \mathrm{FBW})^2 + 4}}{2}. \quad (5)$$

Fig. 1 shows some typical frequency responses of this type of filters as compared to that of a Chebyshev filter. Note that the figure does not show the return loss L_R that is evaluated at -20 dB. As can be seen, the improvement in selectivity over the Chebyshev filter is evident. The closer the attenuation poles to the cutoff frequency ($\Omega = 1$), the sharper the filter skirt and the higher the selectivity.

To realize this type of filtering characteristics in microstrip, we have developed the filter configurations shown in Fig. 2. The filters are comprised of even numbers of microstrip open-loop resonators. Each of the open-loop resonators has a perimeter about a half-wavelength. Note that the shape of resonators need not be square; it may be rectangular, circular, or a meander open-loop, thus, it can be adapted for different substrate sizes. However, for the smaller size of the loop, the unloaded quality factor of the resonator could be decreased due to higher conductor losses. Although only the filters up to degree $N = 8$ are illustrated, the building up of filters with a higher degree based on the coupled open-loop resonators is feasible. A general coupling structure for this class of filters is depicted in Fig. 3, where each node represents a resonator, the full lines indicate the main path couplings, and the broken line denotes the cross coupling. It is essential that the sign of cross coupling

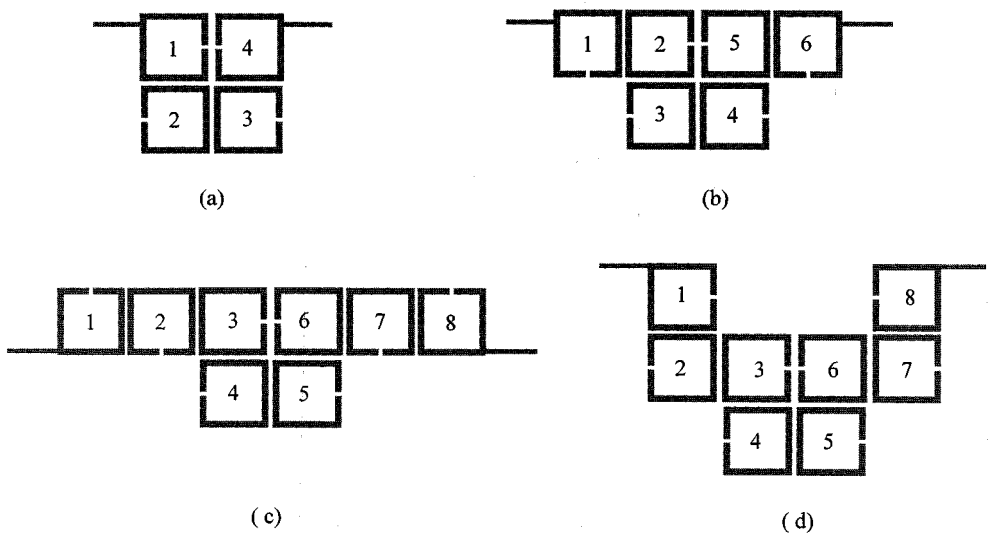

Fig. 2. Configurations of microstrip bandpass filters exhibiting a single pair of attenuation poles at finite frequencies.

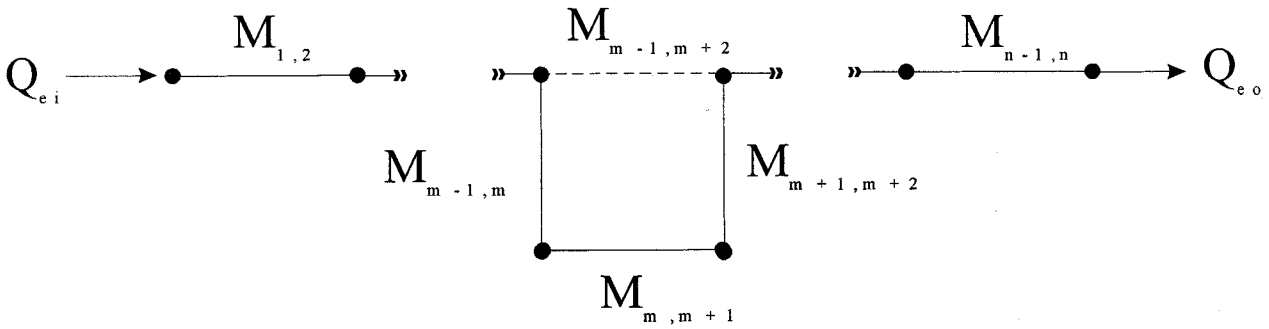

Fig. 3. General coupling structure of the bandpass filters with a single pair of attenuation poles at finite frequencies.

$M_{m-1,\,m+2}$ be opposite to that of $M_{m,\,m+1}$ in order to realize a pair of attenuation poles at finite frequencies, where $m = N/2$ with N being the degree of the filter. This simply implies that $M_{m,\,m+1}$ and $M_{m-1,\,m+2}$ are out-of-phase. In Fig. 2, the cross coupling $M_{m-1,\,m+2}$ is the electric coupling while the coupling $M_{m,\,m+1}$ is the magnetic coupling. This is obvious because, at resonance, the electric fringe field is much stronger near the open gaps of resonators $m-1$ and $m+2$, whereas the magnetic fringe field is much stronger opposite to the gaps of resonators m and $m+1$. It can be shown by the full-wave electromagnetic (EM) simulation that these two types of couplings are indeed out-of-phase. It should be remarked that to realize a single pair of attenuation poles, the cross coupling need not necessarily be electric coupling, and it is possible to use the magnetic coupling for $M_{m-1,\,m+2}$ with the electric coupling for $M_{m,\,m+1}$, as long as they are out-of-phase.

III. Design Technique

The design parameters of bandpass filters, i.e., the coupling coefficients and external quality factor in Fig. 3, can be determined in terms of circuit elements of a low-pass prototype filter of Fig. 4, which consists of lumped capacitors and ideal admittance inverters. The relationships between the bandpass design parameters and the low-pass elements are

$$\begin{aligned} Q_{ei} &= Q_{eo} \\ &= \frac{C_1}{\mathrm{FBW}} \\ M_{n,\,n-1} &= M_{N-n,\,N-n+1} \\ &= \frac{\mathrm{FBW}}{\sqrt{C_n C_{n+1}}}, \qquad \text{for } n = 1 \text{ to } \frac{N}{2} \\ M_{m,\,m+1} &= \frac{\mathrm{FBW} \cdot J_m}{C_m}, \qquad \text{for } m = \frac{N}{2} \\ M_{m-1,\,m+2} &= \frac{\mathrm{FBW} \cdot J_{m-1}}{C_{m-1}}, \qquad \text{for } m = \frac{N}{2} \end{aligned} \tag{6}$$

where FBW denotes the fractional bandwidth of the bandpass filter, C is the capacitance of the lumped capacitor and J is the characteristic admittance of the inverter, and N is the degree of the filter.

To find the element values of a low-pass prototype, one may use an approximate synthesis method described in [2]. This method is simple, but it suffers from inaccuracy and can even fail for highly selective filters that require to move the attenuation poles closer to the cutoff frequencies of the passband. This necessitates the use of an exact synthesis, as

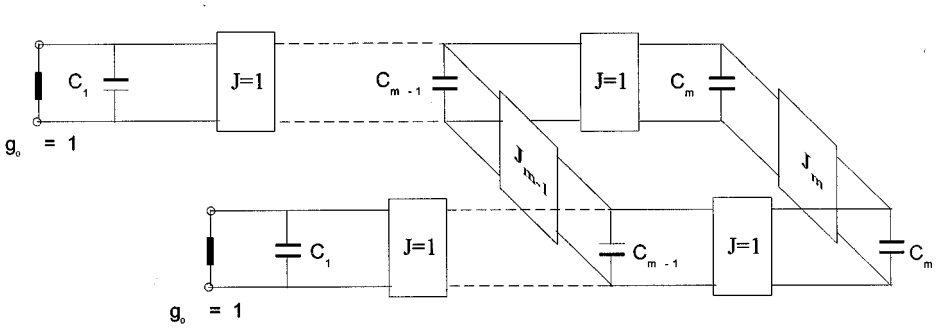

Fig. 4. Low-pass prototype for the filter synthesis.

TABLE I
ELEMENT VALUES OF A FOUR-POLE PROTOTYPE ($L_R = -20$ dB)

Ω_a	C_1	C_2	J_1	J_2
1.80	0.95974	1.42192	-0.21083	1.11769
1.85	0.95826	1.40972	-0.19685	1.10048
1.90	0.95691	1.39927	-0.18429	1.08548
1.95	0.95565	1.39025	-0.17297	1.07232
2.00	0.95449	1.38235	-0.16271	1.06062
2.05	0.95341	1.37543	-0.15337	1.05022
2.10	0.95242	1.36934	-0.14487	1.04094
2.15	0.95148	1.36391	-0.13707	1.03256
2.20	0.95063	1.35908	-0.12992	1.02499
2.25	0.94982	1.35473	-0.12333	1.0181
2.30	0.94908	1.35084	-0.11726	1.01187
2.35	0.94837	1.3473	-0.11163	1.00613
2.40	0.94772	1.34408	-0.10642	1.00086

TABLE II
ELEMENT VALUES OF A SIX-POLE PROTOTYPE ($L_R = -20$ dB)

Ω_a	C_1	C_2	C_3	J_2	J_3
1.20	1.01925	1.45186	2.47027	-0.39224	1.95202
1.25	1.01642	1.44777	2.30923	-0.33665	1.76097
1.30	1.01407	1.44419	2.21	-0.29379	1.63737
1.35	1.01213	1.44117	2.14383	-0.25976	1.55094
1.40	1.01051	1.43853	2.09713	-0.23203	1.487
1.45	1.00913	1.43627	2.0627	-0.20901	1.43775
1.50	1.00795	1.4343	2.03664	-0.18962	1.39876
1.55	1.00695	1.43262	2.01631	-0.17308	1.36714
1.60	1.00606	1.43112	2.00021	-0.15883	1.34103

TABLE III
ELEMENT VALUES OF AN EIGHT-POLE PROTOTYPE ($L_R = -20$ dB)

Ω_a	C_1	C_2	C_3	C_4	J_3	J_4
1.20	1.02947	1.46854	1.99638	1.96641	-0.40786	1.4333
1.25	1.02797	1.46619	1.99276	1.88177	-0.35062	1.32469
1.30	1.02682	1.46441	1.98979	1.82834	-0.30655	1.25165
1.35	1.02589	1.46295	1.98742	1.79208	-0.27151	1.19902
1.40	1.02514	1.46179	1.98551	1.76631	-0.24301	1.15939
1.45	1.02452	1.46079	1.98385	1.74721	-0.21927	1.12829
1.50	1.024	1.45995	1.98246	1.73285	-0.19928	1.10347
1.55	1.02355	1.45925	1.98122	1.72149	-0.18209	1.08293
1.60	1.02317	1.45862	1.98021	1.71262	-0.16734	1.06597

pointed out in [2]. However, the exact synthesis process is rather complicated and time consuming because there does not exist any closed-form formulas for the element values. An alternative synthesis approach recently reported in [12] would still need much effort to implement. To circumvent the difficulties, we have tabulated a set of design data in Tables I–III. The values of the attenuation pole frequency Ω_a were chosen such that they cover a wide range of practical designs for selective microstrip bandpass-filter responses. Referring to Fig. 1, the sidelobe at the stopband would be too high if Ω_a is smaller than the given values. For the less selective filter, in which Ω_a is larger than the given values, the element values of the filter may be obtained using the approximate synthesis method described in [2].

An approximate synthesis may be carried out using the following explicit formulas, which are obtained by curve fitting for $L_R = -20$ dB:

$$\begin{aligned}
C_1(\Omega_a) &= 1.22147 - 0.35543 \cdot \Omega_a + 0.18337 \cdot \Omega_a^2 \\
&\quad - 0.0447 \cdot \Omega_a^3 + 0.00425 \cdot \Omega_a^4 \\
C_2(\Omega_a) &= 7.22106 - 9.48678 \cdot \Omega_a + 5.89032 \cdot \Omega_a^2 \\
&\quad - 1.65776 \cdot \Omega_a^3 + 0.17723 \cdot \Omega_a^4 \\
J_1(\Omega_a) &= -4.30192 + 6.26745 \cdot \Omega_a - 3.67345 \cdot \Omega_a^2 \\
&\quad + 0.9936 \cdot \Omega_a^3 - 0.10317 \cdot \Omega_a^4 \\
J_2(\Omega_a) &= 8.17573 - 11.36315 \cdot \Omega_a + 6.96223 \cdot \Omega_a^2 \\
&\quad - 1.94244 \cdot \Omega_a^3 + 0.20636 \cdot \Omega_a^4, \\
&\quad \text{for } N = 4 \text{ and } 1.8 \le \Omega_a \le 2.4
\end{aligned} \tag{7}$$

$$\begin{aligned}
C_1(\Omega_a) &= 1.70396 - 1.59517 \cdot \Omega_a + 1.40956 \cdot \Omega_a^2 \\
&\quad - 0.56773 \cdot \Omega_a^3 + 0.08718 \cdot \Omega_a^4 \\
C_2(\Omega_a) &= 1.97927 - 1.04115 \cdot \Omega_a + 0.75297 \cdot \Omega_a^2 \\
&\quad - 0.245447 \cdot \Omega_a^3 + 0.02984 \cdot \Omega_a^4 \\
C_3(\Omega_a) &= 151.54097 - 398.03108 \cdot \Omega_a + 399.30192 \cdot \Omega_a^2 \\
&\quad - 178.6625 \cdot \Omega_a^3 + 30.04429 \cdot \Omega_a^4 \\
J_2(\Omega_a) &= -24.36846 + 60.76753 \cdot \Omega_a - 58.32061 \cdot \Omega_a^2 \\
&\quad + 25.23321 \cdot \Omega_a^3 - 4.131 \cdot \Omega_a^4 \\
J_3(\Omega_a) &= 160.91445 - 422.57327 \cdot \Omega_a + 422.48031 \cdot \Omega_a^2 \\
&\quad - 188.6014 \cdot \Omega_a^3 + 31.66294 \cdot \Omega_a^4, \\
&\quad \text{for } N = 6 \text{ and } 1.2 \le \Omega_a \le 1.6
\end{aligned} \tag{8}$$

$$\begin{aligned}
C_1(\Omega_a) &= 1.64578 - 1.55281 \cdot \Omega_a + 1.48177 \cdot \Omega_a^2 \\
&\quad - 0.63788 \cdot \Omega_a^3 + 0.10396 \cdot \Omega_a^4 \\
C_2(\Omega_a) &= 2.50544 - 2.64258 \cdot \Omega_a + 2.55107 \cdot \Omega_a^2 \\
&\quad - 1.11014 \cdot \Omega_a^3 + 0.18275 \cdot \Omega_a^4
\end{aligned}$$

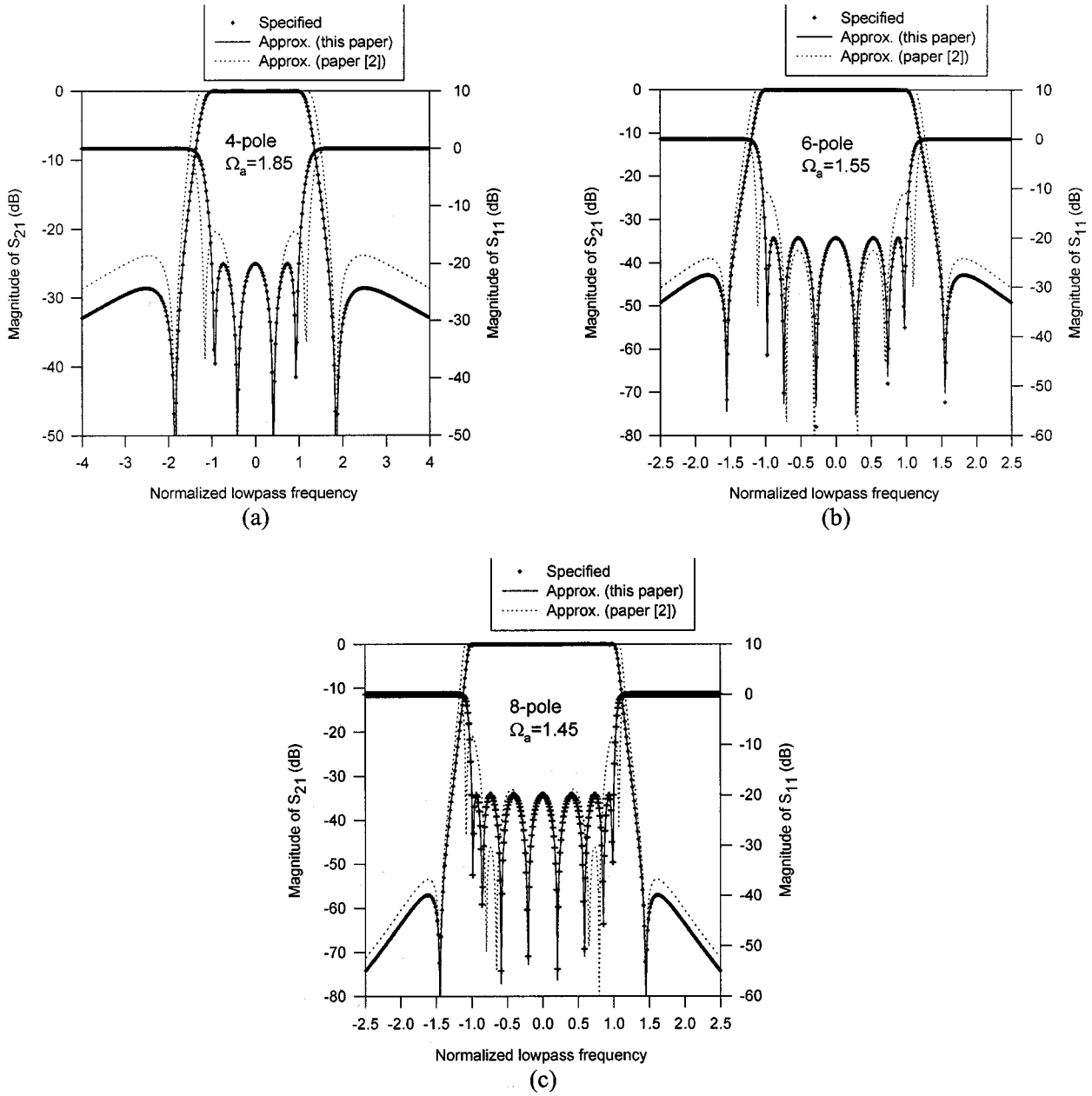

Fig. 5. Comparison of specified filter responses (+) with those obtained using the approximate synthesis of this paper (solid line) and the approximate synthesis [2] (dotted line).

$$
\begin{aligned}
C_3(\Omega_a) &= 3.30522 - 3.25128 \cdot \Omega_a + 3.06494 \cdot \Omega_a^2 \\
&\quad - 1.30769 \cdot \Omega_a^3 + 0.21166 \cdot \Omega_a^4 \\
C_4(\Omega_a) &= 75.20324 - 194.70214 \cdot \Omega_a + 194.55809 \cdot \Omega_a^2 \\
&\quad - 86.76247 \cdot \Omega_a^3 + 14.54825 \cdot \Omega_a^4 \\
J_3(\Omega_a) &= -25.42195 + 63.50163 \cdot \Omega_a - 61.03883 \cdot \Omega_a^2 \\
&\quad + 26.44369 \cdot \Omega_a^3 - 4.3338 \cdot \Omega_a^4 \\
J_4(\Omega_a) &= 82.26109 - 213.43564 \cdot \Omega_a + 212.16473 \cdot \Omega_a^2 \\
&\quad - 94.28338 \cdot \Omega_a^3 + 15.76923 \cdot \Omega_a^4, \\
&\quad \text{for } N = 8 \text{ and } 1.2 \le \Omega_a \le 1.6.
\end{aligned} \tag{9}
$$

These formulas are very easy for programming, finding the element values in merely a fraction of a second.

After the finding of element values for a low-pass prototype, the frequency response can be calculated by

$$
\begin{aligned}
S_{21}(\Omega) &= \frac{Y_o(\Omega) - Y_e(\Omega)}{\big(1 + Y_e(\Omega)\big) \cdot \big(1 + Y_o(\Omega)\big)} \\
S_{11}(\Omega) &= \frac{1 - Y_e(\Omega) \cdot Y_o(\Omega)}{\big(1 + Y_e(\Omega)\big) \cdot \big(1 + Y_o(\Omega)\big)}
\end{aligned} \tag{10}
$$

where Y_e and Y_o are the even- and odd-mode input admittance of the filter in Fig. 4, which can easily be expressed in terms of the elements in a ladder structure as follows:

$$
Y_e(\Omega) = j(\Omega C_1 + J_1) + \frac{1}{j(\Omega C_2 + J_2)}
$$

$$Y_o(\Omega) = j(\Omega C_1 - J_1) + \frac{1}{j(\Omega C_2 - J_2)}, \qquad \text{for } N = 4 \tag{11}$$

$$Y_e(\Omega) = j\Omega C_1 + \cfrac{1}{j(\Omega C_2 + J_2) + \cfrac{1}{j(\Omega C_3 + J_3)}}$$
$$Y_o(\Omega) = j\Omega C_1 + \cfrac{1}{j(\Omega C_2 - J_2) + \cfrac{1}{j(\Omega C_3 - J_3)}},$$
$$\text{for } N = 6 \tag{12}$$

$$Y_e(\Omega) = j\Omega C_1 + \cfrac{1}{j\Omega C_2 + \cfrac{1}{j(\Omega C_3 + J_3) + \cfrac{1}{j(\Omega C_4 + J_4)}}}$$
$$Y_o(\Omega) = j\Omega C_1 + \cfrac{1}{j\Omega C_2 + \cfrac{1}{j(\Omega C_3 - J_3) + \cfrac{1}{j(\Omega C_4 - J_4)}}},$$
$$\text{for } N = 8. \tag{13}$$

The frequency locations of a pair of attenuation poles can be determined by imposing the condition of $|S_{21}(\Omega)| = 0$ upon (10). This requires $|Y_o(\Omega) - Y_e(\Omega)| = 0$ or $Y_o(\Omega) = Y_e(\Omega)$ for $\Omega = \pm\Omega_a$. From (11)–(13), we have

$$j(\Omega_a C_{m-1} + J_{m-1}) + \frac{1}{j(\Omega_a C_m + J_m)} = j(\Omega_a C_{m-1} - J_{m-1}) + \frac{1}{j(\Omega_a C_m - J_m)}, \qquad \text{for } m = \frac{N}{2}. \tag{14}$$

This leads to

$$\Omega_a = \frac{1}{C_m}\sqrt{J_m^2 - \frac{J_m}{J_{m-1}}}, \qquad \text{for } m = \frac{N}{2}. \tag{15}$$

As an example, from Table II where $m = 3$, we have $C_3 = 2.47027$, $J_2 = -0.39224$, and $J_3 = 1.95202$ for $\Omega_a = 1.20$. Substituting these element values into (15) yields $\Omega_a = 1.19998$, an excellent match. This would prove the numerical accuracy of the design data presented. It is also interesting to note from (15) that even if J_m and J_{m-1} exchange signs, the locations of attenuation poles are not changed. This is because the signs of these two characteristic admittances decide the signs of $M_{m,m+1}$ and $M_{m-1,m+2}$, as referred to (6), respectively. This is the reason why we have pointed out in Section II that the signs for $M_{m,m+1}$ and $M_{m-1,m+2}$ are relative.

To demonstrate the accuracy of the proposed approximate synthesis technique, Fig. 5 shows the comparison of the specified filter response with those obtained using Levy's [2] and our approximate designs. The approximate designs as proposed in (7)–(9) are so accurate that their responses coincide with the specified ones. On the contrary, the filter responses resulting from Levy's approximate designs are not quite satisfactory for the highly selective filters, as the return loss has deteriorated to a great extent, the passband cutoff frequency has increased and the stopband attenuation has decreased as well.

IV. Full-Wave EM Simulations

The next step of the filter design is to characterize the couplings and external quality factor in terms of physical structures so that the physical dimensions of the filter can be determined against the design parameters of (6). There are four different types of coupling structures encountered in the filter design. These couplings may be referred to as the magnetic coupling, electric coupling, mixed coupling, and hybrid coupling, respectively. As far as the coupling between any pair of coupled resonators is concerned, it is quite easy to identify in the full-wave EM simulation the two split resonant frequencies f_{p1} and f_{p2}, which is related to the coupling coefficient as [7]

$$M_{i,j} = \frac{f_{p2}^2 - f_{p1}^2}{f_{p2}^2 + f_{p1}^2}. \tag{16}$$

The external quality factor can be modeled by

$$Q_e = \frac{f_0}{\delta f_{3\,\mathrm{dB}}} \tag{17}$$

where f_0 and $\delta f_{3\,\mathrm{dB}}$ are the resonant frequency and the 3-dB bandwidth of the input or output resonator when it alone is externally excited. Shown in Fig. 6 are the typical simulation results obtained using a full-wave EM simulator [13]. In order to allow readers to more accurately reproduce and use the curves, a few data points are listed in the figure as pairs of axis values.

V. Design Examples

A. Six-Pole Filter Design Example

The first filter example is designed against the following specifications:

Center frequency	955 MHz;
Fractional bandwidth FBW	7.331%;
40-dB rejection bandwidth	105 MHz;
Passband return loss	−20 dB.

These specifications can be fulfilled by a six-pole filter with a pair of attenuation poles at $\Omega = \pm\Omega_a = \pm 1.5$. It might be mentioned that the number of poles and Ω_a could be obtained by directly optimizing the transfer function of (1). The theoretical response of the filter is shown in Fig. 7. From Table II, we can find the element values for $\Omega_a = 1.5$, namely, $C_1 = 1.00795$, $C_2 = 1.4343$, $C_3 = 2.03664$, $J_2 = -0.18962$, and $J_3 = 1.39876$. Substituting these element values and the FBW into (6) results in the design parameters for the bandpass filter, i.e.,

$$\begin{aligned} M_{1,2} &= 0.06097 \\ M_{2,3} &= 0.04289 \\ M_{3,4} &= 0.05035 \\ M_{2,5} &= -0.00969 \\ Q_{ei} &= Q_{eo} \\ &= 13.74928. \end{aligned} \tag{18}$$

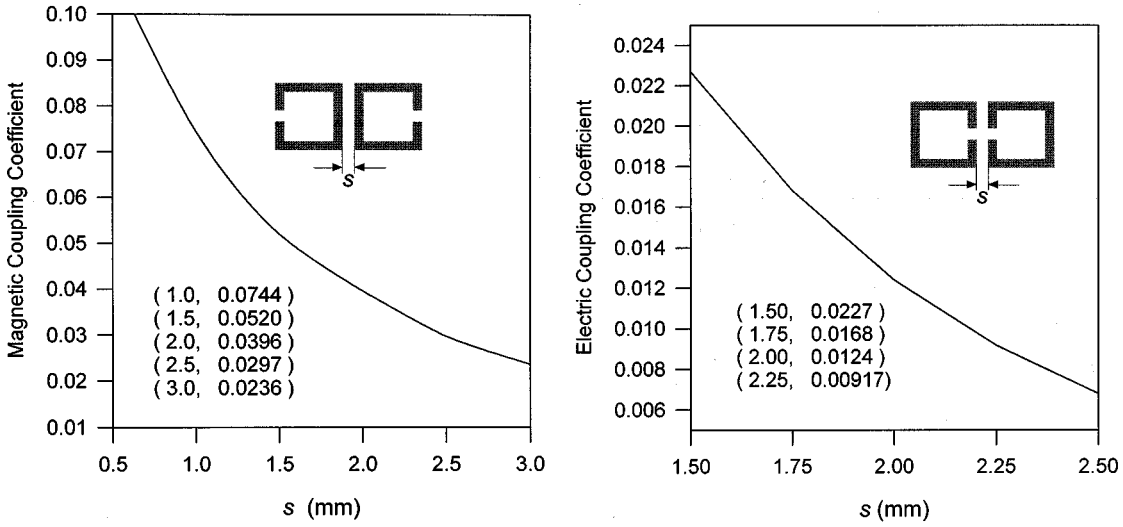

(a)

(b)

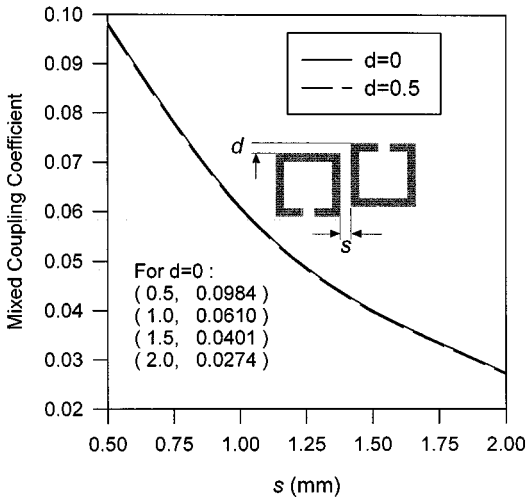

(c)

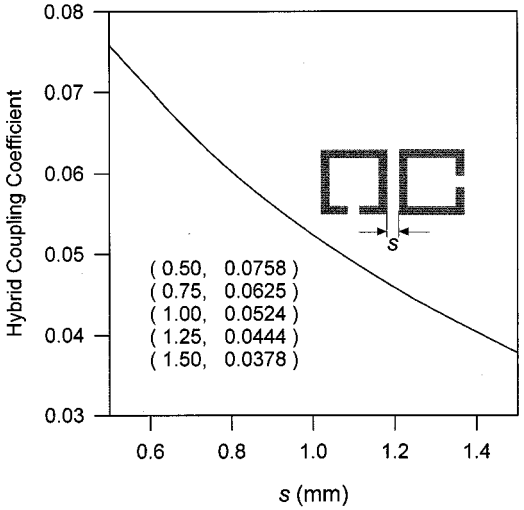

(d)

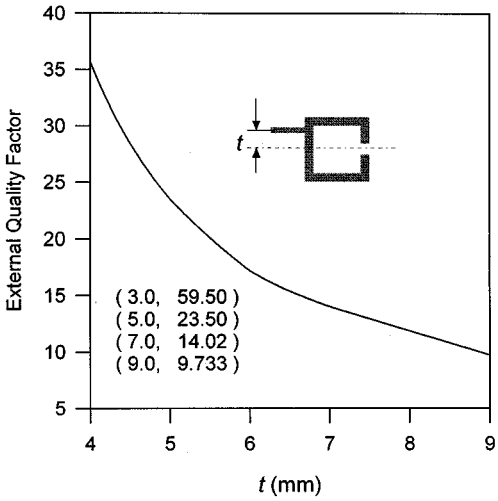

(e)

Fig. 6. Full-wave EM simulations. (a) Magnetic coupling. (b) Electric coupling. (c) Mixed coupling. (d) Hybrid coupling. (e) External quality factor. (All resonators have a line width of 1.5 mm and a size of 16 mm $\times$ 16 mm on the substrate with a relative dielectric constant of 10.8 and a thickness of 1.27 mm.)

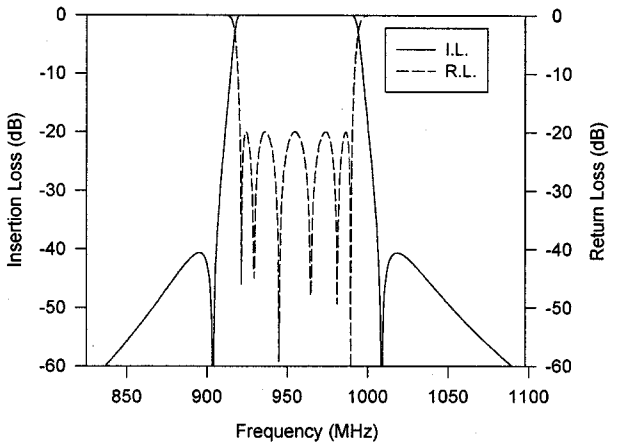

Fig. 7. The theoretical response of the six-pole microstrip filter with a pair of attenuation poles.

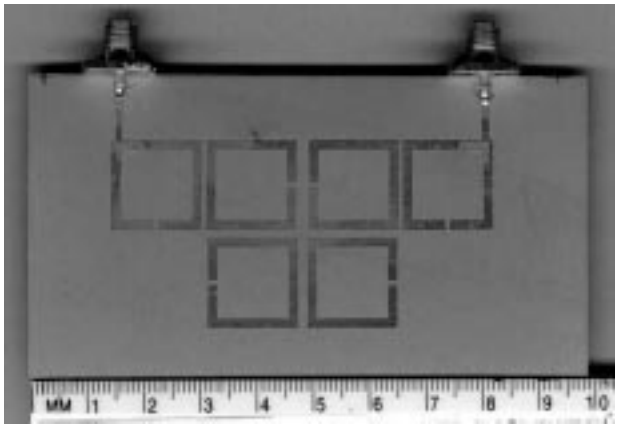

Fig. 8. Fabricated six-pole microstrip bandpass filter with a single pair of attenuation poles at finite frequencies (note: the small divisions in the scale are millimeters and the numbers are centimeters).

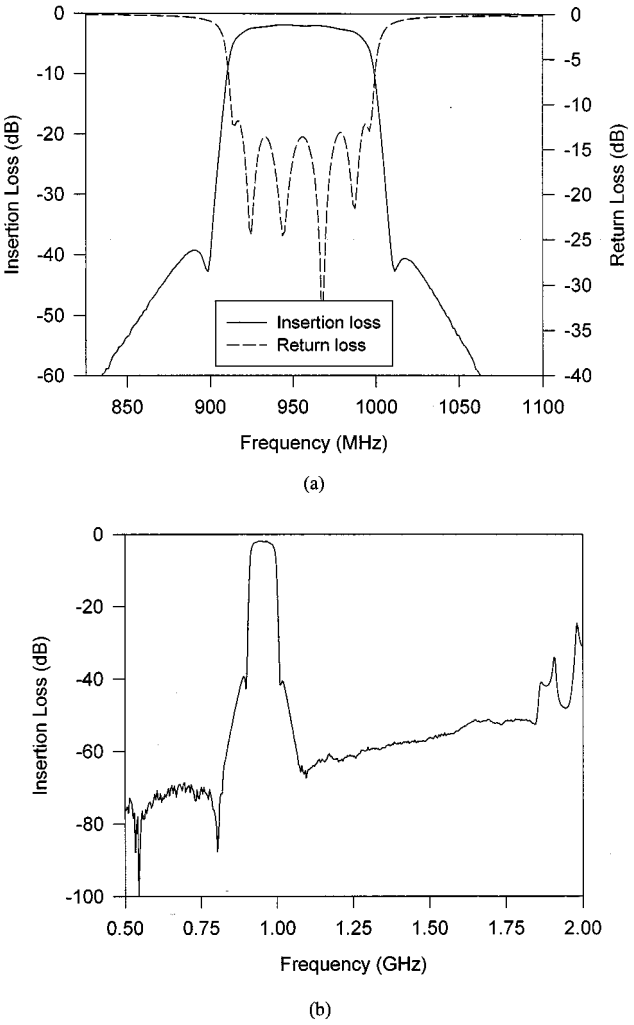

Fig. 9. Measured performance of the six-pole microstrip filter. (a) Insertion and return losses. (b) Spurious response of the six-pole microstrip filter.

The filter is realized using the configuration of Fig. 2(b) and fabricated using a copper microstrip on an RT/Duroid substrate with a relative dielectric constant of 10.8 and a thickness of 1.27 mm. The filter dimensions are determined based on the full-wave EM simulation results presented in the previous section. $M_{1,2}$ is realized with a hybrid coupling in Fig. 6(d). $M_{2,3}$ is realized with a mixed coupling in Fig. 6(c). $M_{3,4}$ is realized with a magnetic coupling in Fig. 6(a), while the cross coupling $M_{2,5}$ is realized with an electric coupling in Fig. 6(b). Fig. 8 is a photograph of the fabricated filter. The size of the filter is about $0.55\lambda_{g0}$ by $0.28\lambda_{g0}$, where λ_{g0} is the guided wavelength of 50-Ω line on the substrate at the midband frequency. The filter is measured on an HP8510 network analyzer. The measured performance is shown in Fig. 9. The midband insertion loss is about -2.0 dB, which is mainly due to the conductor loss of copper. The two attenuation poles near the cutoff frequencies of the passband can clearly be identified. The first higher order mode spurious response occurs at about $2\omega_0$, which is expected for this class of filters because the perimeter of each resonator is about a half-wavelength. It should be mentioned that, in order to compensate for fabrication errors, tuning is required. The errors normally caused the frequency to shift and a large ripple to appear in the passband. The tuning was done by trimming or using some tuning elements. It was found that the tuning of the open gap of each open-loop resonator was more effective.

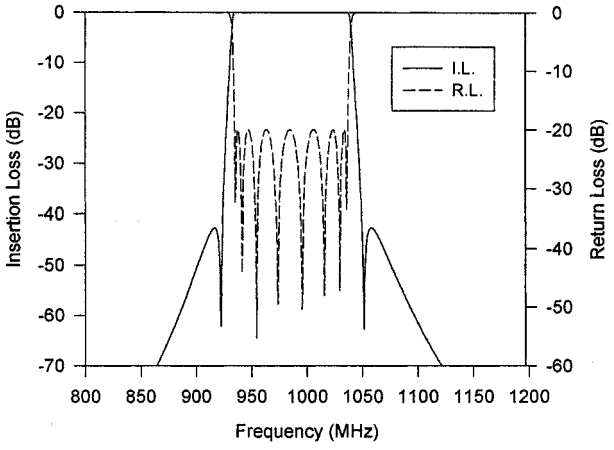

Fig. 10. Theoretical performance of the eight-pole microstrip filter with a single pair of attenuation poles.

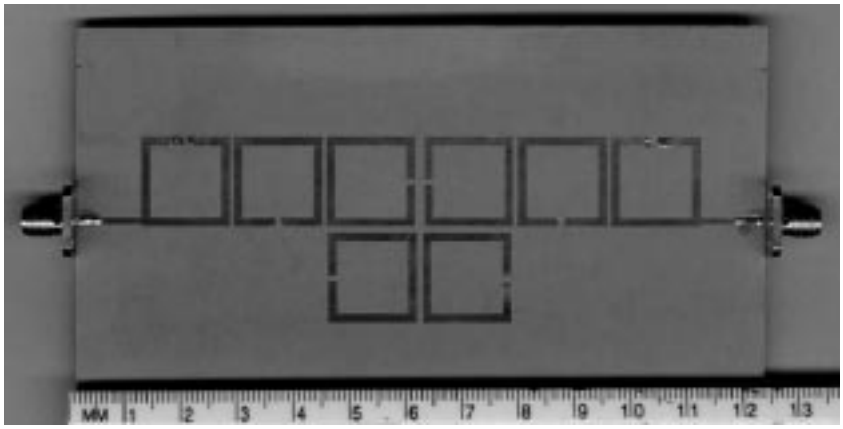

Fig. 11. Fabricated eight-pole microstrip bandpass filter with a single pair of attenuation poles at finite frequencies (note: the small divisions in the scale are millimeters and the numbers are centimeter).

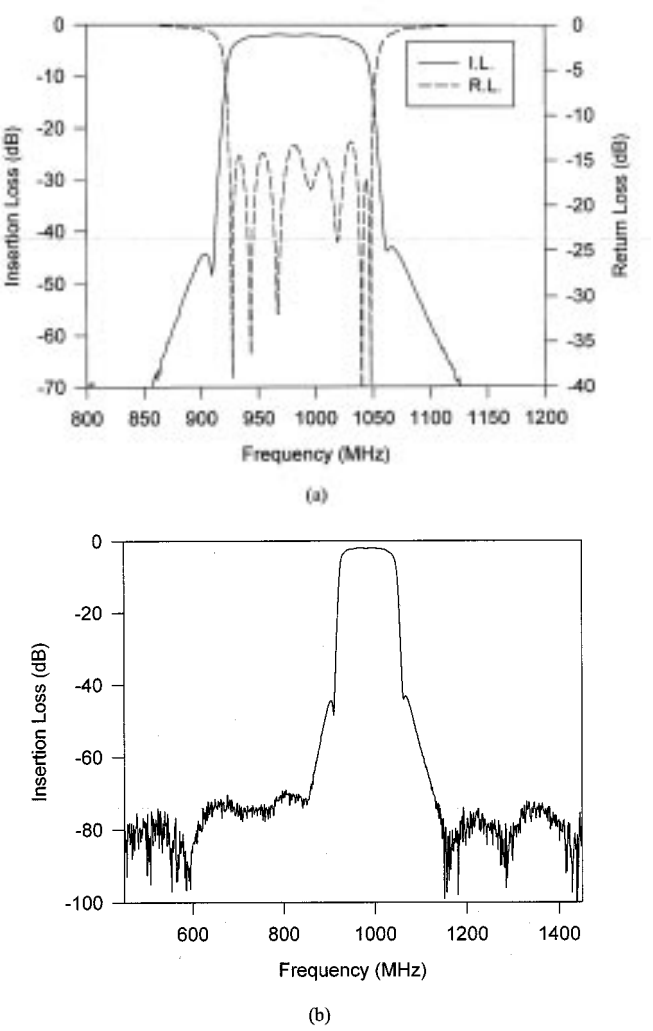

Fig. 12. Measured performance of the eight-pole microstrip filter. (a) Insertion and return losses. (b) Wide-band response.

B. Eight-Pole Filter Design Example

The second filter example is an eight-pole filter, which is aimed to meet the following specifications:

Center frequency	985 MHz;
Fractional bandwidth FBW	10.359%;
40-dB rejection bandwidth	125.5 MHz;
Passband return loss	-20 dB.

The pair of attenuation poles are placed at $\Omega = \pm 1.2645$ in order to meet the rejection specification. The element values of the low-pass prototype can be obtained by substituting $\omega_a = 1.2645$ into (9). This results in $C_1 = 1.02761$, $C_2 = 1.46561$, $C_3 = 1.99184$, $C_4 = 1.86441$, $J_3 = -0.33681$, and $J_4 = 1.3013$. The theoretical response of the filter, calculated using (10) together with the frequency mapping of (5), is shown in Fig. 10. The design parameters of this bandpass filter are

$$\begin{aligned} M_{1,2} &= 0.08441 \\ M_{2,3} &= 0.06063 \\ M_{3,4} &= 0.05375 \\ M_{4,5} &= 0.0723 \\ M_{3,6} &= -0.01752 \\ Q_{ei} &= Q_{eo} \\ &= 9.92027 \end{aligned} \tag{19}$$

according to (6). The filter is realized using the configuration of Fig. 2(c) and fabricated using a copper microstrip on an RT/Duroid substrate with a relative dielectric constant of 10.8 and a thickness of 1.27 mm. Fig. 11 is a photograph of the fabricated filter. The size of the filter amounts to $0.87\lambda_{g0}$ by $0.29\lambda_{g0}$. The measured performance is shown in Fig. 12, obtained from the HP8510 network analyzer. The midband insertion loss is about -2.1 dB, which, again, is attributed to the conductor loss of copper. The two attenuation poles near the cutoff frequencies of the passband are observable, which improve the selectivity.

VI. Conclusion

We have presented the design of a class of selective microstrip bandpass filters that exhibit a single pair of attenuation poles at finite frequencies. This class of filters is able to improve the selectivity while maintaining a lower insertion loss. The use of microstrip open-loop resonators not only allows the cross coupling to be realized, but also makes the filters compact. We have introduced a practical design technique, including the tabulated design data and formulas for accurate and fast filter synthesis.

This design technique is, of course, not limited to the application of microstrip filters and, hence, it can be applied to design a filter using other transmission-line media. The full-wave EM simulations have been carried out to determine the filter dimensions. The compact size and the excellent performance of this type of filter have been demonstrated by the two filter design examples with both the theoretical and experimental results.

REFERENCES

[1] R. M. Kurzok, "General four-resonator filters at microwave frequencies," *IEEE Trans. Microwave Theory Tech.*, vol. MTT-14, pp. 295–296, July 1966.

[2] R. Levy, "Filters with single transmission zeros at real and imaginary frequencies," *IEEE Trans. Microwave Theory Tech.*, vol. MTT-24, pp. 172–181, Apr. 1976.

[3] M. J. Lancaster, *Passive Microwave Device Applications of Superconductors*. Cambridge, U.K.: Cambridge Univ. Press, 1997.

[4] S. J. Hedges and R. G. Humphreys, "An extracted pole microstrip elliptic function filter using high temperature superconductors," in *Proc. EuMC*, 1994, pp. 517–521.

[5] K. T. Jokela, "Narrow-band stripline or microstrip filters with transmission zeros at real and imaginary frequencies," *IEEE Trans. Microwave Theory Tech.*, vol. MTT-28, pp. 542–547, June 1980.

[6] R. R. Bonetti and A. E. Williams, "New design techniques for coupled-line filters with transmissions zeros," in *Proc. 23rd EuMC*, Madrid, 1993, pp. 240–243.

[7] J.-S. Hong and M. J. Lancaster, "Couplings of microstrip square open-loop resonators for cross-coupled planar microwave filters," *IEEE Trans. Microwave Theory Tech.*, vol. 44, pp. 2099–2109, Nov. 1996.

[8] J.-S. Hong, M. J. Lancaster, R. B. Greed, and D. Jedamzik, "Highly selective microstrip bandpass filters for HTS and other applications," in *28th European Microwave Conf.*, Amsterdam, The Netherlands, Oct. 1998, pp. 1–6.

[9] P. Blondy, A. R. Brown, D. Cross, and G. M. Rebeiz, "Low loss micromachined filters for millimeter-wave telecommunication systems," in *IEEE MTT-S Int. Microwave Symp. Dig.*, Baltimore, MD, June 1998, pp. 1181–1184.

[10] C.-C. Yu and K. Chang, "Novel compact elliptic-function narrow-band bandpass filters using microstrip open-loop resonators with coupled and crossing lines," *IEEE Trans. Microwave Theory Tech.*, vol. 46, pp. 952–958, July 1998.

[11] J. D. Rhodes and S. A. Alseyab, "The generalized Chebyshev low-pass prototype filter," *Circuit Theory Applicat.*, vol. 8, pp. 113–125, 1980.

[12] R. Levy, "Synthesis of general asymmetric singly and doubly termined cross-coupled filters," *IEEE Trans. Microwave Theory Tech.*, vol. 42, pp. 2468–2471, Dec. 1994.

[13] *em Users' Manual*, Sonnet Software Inc., Liverpool, NY, 1996.

Jia-Sheng Hong (M'94) received the D.Phil. degree in engineering science from Oxford University, Oxford, U.K., in 1994.

From 1979 to 1983, he was a Teaching and Research Assistant in radio engineering with Fuzhou University. He then visited Karlsruhe University, where, from 1984 to 1985, he was involved with microwave and millimeter-wave techniques. In 1986, he returned to Fuzhou University, as a Lecturer in microwave communications. In 1990, he became a Graduate Member of St. Peter's College, Oxford University, where he conducted research in EM theory and applications. Since 1994, he has been a Research Fellow at Birmingham University, Birmingham, U.K. His current interests include RF and microwave devices for communications, microwave filters and antennas, microwave applications of high-temperature superconductors, EM modeling, and circuit optimization.

Dr. Hong was the 1983 recipient of a Friedrich Ebert Scholarship and the 1990 recipient of the K. C. Wong Scholarship presented by Oxford University.

Michael J. Lancaster (M'91) received the physics degree and the Ph.D. degree in nonlinear underwater acoustics from Bath University, Bath, U.K., in 1980 and 1984, respectively.

Upon leaving Bath University, he joined the Surface Acoustic Wave (SAW) Group of the Department of Engineering Science, Oxford University, Oxford, U.K., as a Research Fellow, where he was involved in research of the design of new novel SAW devices, including filters and filter banks. These devices worked in the frequency range of 10 MHz–1 GHz. In 1987, he became a Lecturer in the School of Electronic and Electrical Engineering, University of Birmingham, Birmingham, U.K., where he teaches EM theory and microwave engineering. Shortly after joining the School of Electronic and Electrical Engineering, he began the study of the science and applications of high-temperature superconductors, involved mainly with microwave frequencies. He currently heads the Electronic and Materials Devices Group as a Reader. His current personal research interests include microwave filters and antennas, as well as the high-frequency properties and applications of a number of novel and diverse materials.

Dr. Lancaster is currently serving on the IEEE Microwave Theory and Techniques Society (IEEE MTT-S) International Microwave Symposium Technical Committee.